

Measurements of the double layer capacitance

I – INTRODUCTION

All electrochemical processes take place at the electrode/electrolyte interface, *i.e.* the electrical double layer (Figure 1). Different models of this layer were stated by Helmholtz, Gouy-Chapman, Stern, or Grahame [1,2].

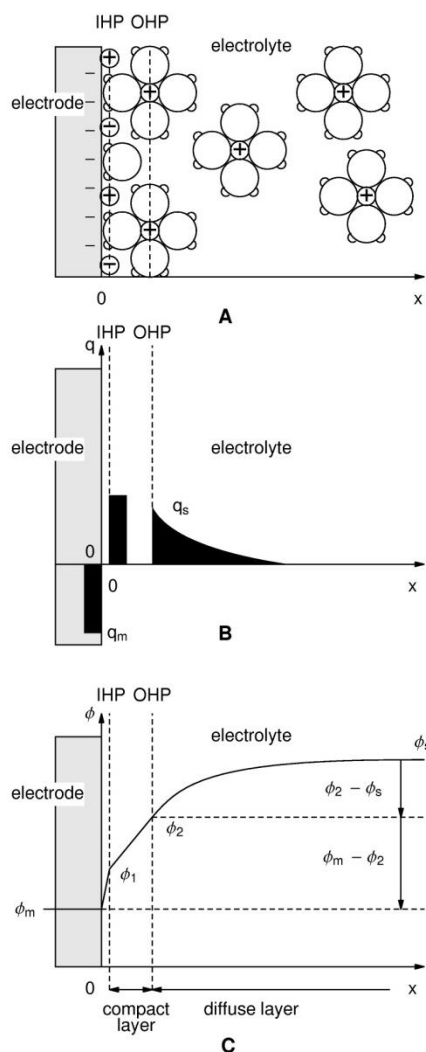


Figure 1: Scheme of the electrical double layer according to the Grahame model (adapted from [2]). IHP: Inner Helmholtz Plane, OHP: Outer Helmholtz Plane. A: Electrode with an excess of negative charge; B: Localization of the charge in excess; C: Potential change versus distance towards the electrode /electrolyte interface.

The structure of the double layer is similar to an electrical condenser constituted by two charged areas separated by a dielectric. The

dielectric thickness corresponds to the ionic radius, *i.e.* 50 nm.

In this note, the electrical double layer of the iron electrode in acidic conditions is investigated. In this purpose, two techniques are used to determine the value of the capacitance: the Electrochemical Impedance Spectroscopy (EIS) and Cyclic Voltammetry (CV).

I – EXPERIMENTAL CONDITIONS

Investigations are performed by the VSP instrument driven by EC-Lab® software in a solution of HCl (0.1 M). The three-electrode set-up is used with:

- a Rotating Disk Electrode (RDE) of iron as a working electrode with a surface area of 3.14 mm²,
- a platinum wire as a counter electrode,
- a Saturated Calomel Electrode (SCE) as a reference electrode.

For both techniques, experiments are carried out at the rotation speed of the electrode: $\Omega = 800$ rpm (rotations per minute). For the CV experiment, the scan rate is 40 mV.s⁻¹.

Data analysis for both techniques is also computed by EC-Lab® software.

III – IMPEDANCE THEORY

The equivalent circuit, described in Figure 2, with a capacitance and a resistance in parallel and an additional resistance corresponding to the ohmic drop ($R_1 + C/R_2$) should be a good model for the double layer. In this case, the resulting Nyquist diagram is close to a perfect semi-circle (Figure 2). However, for real systems, it is hardly ever the case. That's why, a constant phase element (CPE), noted Q in Figure 3, is introduced and used instead of the capacitance C in the $R_1 + Q/R_2$ equivalent circuit [3,4]. Then, the resulting Nyquist diagram (Figure 3) corresponds to a depressed semi-circle in its upper-part.

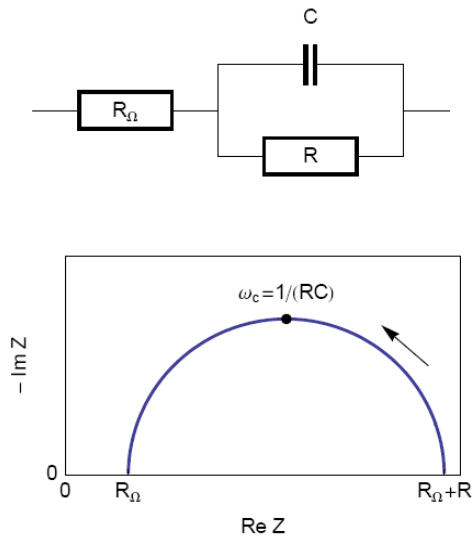


Figure 2: Equivalent electrical circuit $R_{\Omega}+R/C$ (top) and corresponding Nyquist impedance diagram (bottom, arrow indicates increasing angular frequencies).

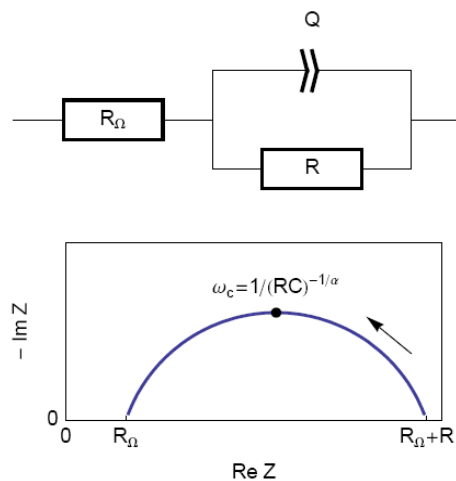


Figure 3: Equivalent electrical circuit $R_{\Omega}+R/Q$ (top) and corresponding Nyquist impedance diagram (bottom, arrow indicates increasing angular frequencies).

Then, the analogy between the relationship described in Figs. 1 and 3 leads to Eq. 1. This equation gives the capacitance value at the frequency corresponding to the apex of the Nyquist diagram.

$$C_{dl} = Q(\omega_c)^{\alpha-1} \quad (1)$$

IV – IMPEDANCE RESULTS AND ANALYSIS

The measurements are carried out with potentiostatic EIS (PEIS) techniques at open circuit voltage E_{oc} in the 100 kHz – 100 mHz frequency range and with a sinus amplitude (V_a) of 10 mV. The settings of the impedance investigation are shown in Figure 4.

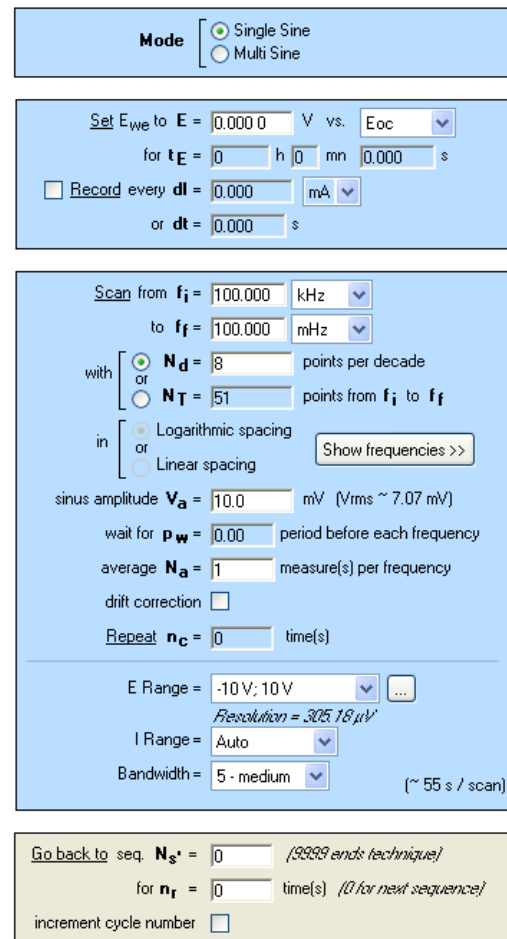


Figure 4: Potentiostatic Impedance “Parameters Settings” window.

Points of the impedance diagram corresponding to lowest frequencies ($Re(Z) \geq 55 \text{ k}\Omega$) clearly show that the system drifts with time, because of the time variant condition [5]. Therefore, these points are not taken into consideration (Figure 5).

As explained above, the fit is performed with the $R1+R2/Q$ equivalent circuit (Fig. 6). First of all, the results show that the ohmic drop resistance ($R1 = R_{\Omega} = 71 \Omega$) is insignificant before the charge transfer resistance

($R_2 = R_t = 58 \text{ k}\Omega$). Moreover the value of Q is $6.3 \mu\text{F}\cdot\text{s}^{\alpha-1}$ with α equal to 0.84.

Then, the capacitance of the system is computed with the “Pseudocapacitance” tool and the value of $5.2 \mu\text{F}$ is determined for C_{dl} (Figure 6) [4].

It is possible to load the settings and the data files as PEIS_CPE.mpr in the EC-Lab® Samples, Fundamental Electrochemistry folder.

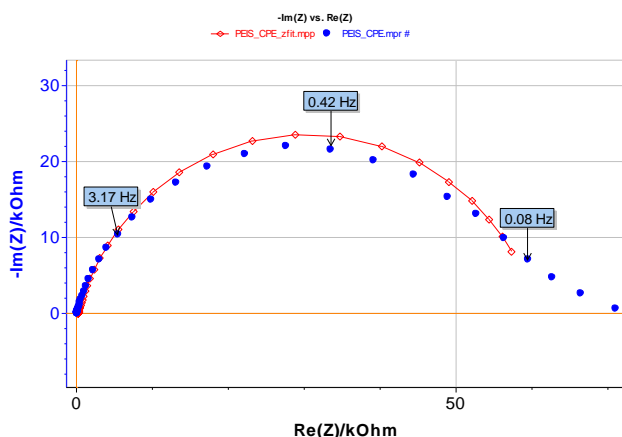


Figure 5: Experimental (blue markers) and fitted (red curve) impedance diagram.

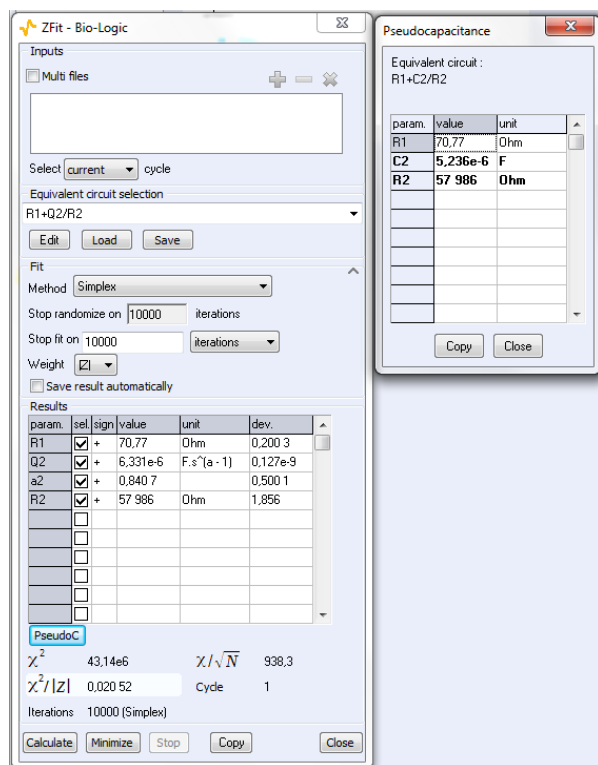


Figure 6: The “ZFit” and “Pseudocapacitance” results.

V – CYCLIC VOLTAMMETRY RESULTS AND ANALYSIS

E_{oc} is determined before starting the CV experiment. The value is -0.235 V vs. SCE . The parameters of the CV technique (Figure 7) are chosen accordingly, *i.e.* in a range of $\pm 15 \text{ mV}$ around E_{oc} with a scan rate of $40 \text{ mV}\cdot\text{s}^{-1}$.

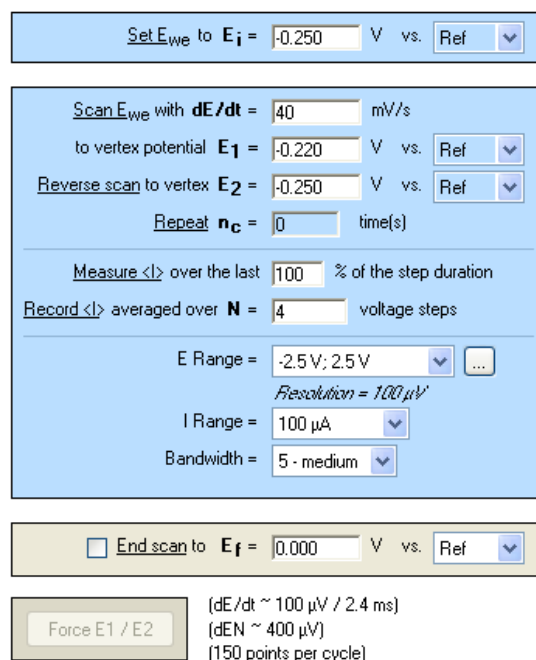


Figure 7: Cyclic Voltammetry “Parameters Settings” window.

As the ohmic drop can be neglected (see previous paragraph), the value of R_p can be determined by calculating the slope of the curve. The R_p values found for forward (Fig. 8) and backward sweeps of the potential are $57 \text{ k}\Omega$ ($= 1/17.673 \times 10^{-6}$) and $61 \text{ k}\Omega$ respectively. Note that the R_p values determined by PEIS or CV techniques are in agreement. As the transport of the material does not limit the kinetics of the redox process, the following Eq. 2 is true [2]:

$$R_p = R_t \quad (2)$$

Assuming our system could be modeled by a real capacitance and a resistance in parallel; we can calculate the equations corresponding to the upper and lower part of the curve around the corrosion potential which is equal

to E_{oc} . From these equations, we extrapolated the two current values I_a and I_c corresponding to the corrosion potential for the anodic and the cathodic part of the curve, respectively, and were able to calculate the double layer capacitance with the following equation:

$$\frac{I_a - I_c}{2} = C_{dl} \frac{dE}{dt} \quad (3)$$

Finally, considering the values given in Figure 8 and Eq. 3, the capacitance, C_{dl} , is $4.3 \mu\text{F}$. It is possible to load the settings and the data files as CV_CPE.mpr in the EC-Lab® Samples folder.

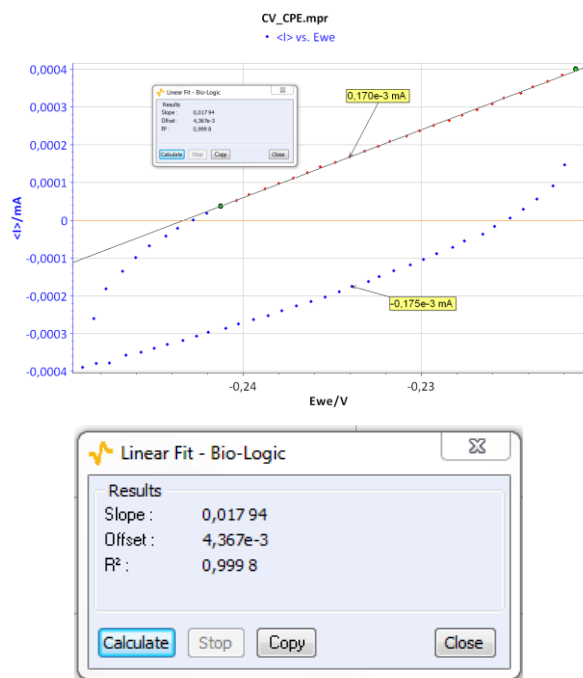


Figure 8: CV curve I vs. E_{we} for forward and backward voltage scan (top). “Linear Fit” tool for determining R_p (bottom).

By the way, it is possible to simulate the CV response of a circuit R/Q (Figure 3). For that purpose, the relationship Eq. (4), which expresses the current response of an R/Q circuit to a linear change of potential, is used:

$$I(t) = \frac{v_b t}{R2} + \frac{Q v_b t^{1-\alpha}}{\Gamma(2-\alpha)} \quad (4)$$

where v_b is the scan rate of the electrode potential, Γ the Euler gamma function, α the dispersion parameter of the CPE and s the Laplace variable.

Figure 9 shows the experimental data points and the data simulated using Eq. 4. The results of the data fitting on the experimental points gives a value of $8.2 \mu\text{F}\cdot\text{s}^{\alpha-1}$ with $\alpha = 0.841$ determined by EIS.

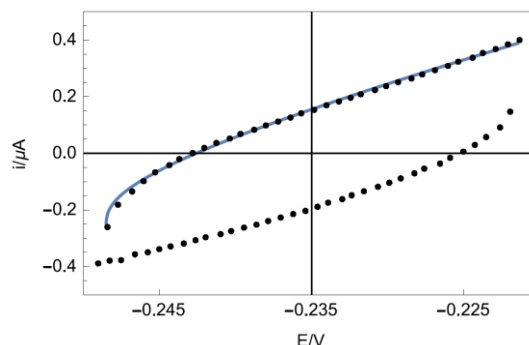


Figure 9: Experimental points (dots) and Simulation (line) of the CV response of circuit R+R/Q (Figure 3) plotted by Mathematica software.

VI – CONCLUSION

In this note, we have shown how to calculate capacitance values using EIS and CV. First, it was assumed that the double layer was a true capacitance, and secondly it was a constant phase element (CPE). In this case, a pseudo capacitance was calculated and compared to the true capacitance value. All these values are summarized in Table I. The values given by all assumptions and all methods were all of the same order of magnitude.

The values given by all assumptions and all methods were all of the same order of magnitude.

Table I: Summary

| EIS | | CV | |
|----------------------|---|----------------------|---|
| C_{dl} | CPE | C_{dl} | CPE |
| $C_{dl}/\mu\text{F}$ | $Q/\mu\text{F}\cdot\text{s}^{\alpha-1}$ | $C_{dl}/\mu\text{F}$ | $Q/\mu\text{F}\cdot\text{s}^{\alpha-1}$ |
| 5.2 | 6.3 | 4.3 | 8.2 |

Data files can be found in :

C:\Users\xxx\Documents\EC-Lab\Data\Samples\Fundamental Electrochemistry\technique_CPE

REFERENCES

- 1) A. J. Bard, L. R. Faulkner, *Electrochemical methods. Fundamentals and applications*, Wiley, Hoboken, (2001).
- 2) J.-P. Diard, B. Le Gorrec, C. Montella *Cinétique électrochimique*, Hermann, Paris, (1996).
- 3) E. Barsoukov, J.R. Macdonald, *Impedance Spectroscopy. Theory, experiment and applications.*, Wiley, Hoboken, (1987).
- 4) [Application Note #20](#) “Pseudo capacitance calculation”
- 5) [Application Note #55](#) “Interpretation problems of impedance measurements made on time variant systems”

Revised in 07/2018